Mem. S.A.It. Vol. 84, 568

Memorie della

The X-ray properties of the Fermi/*LAT* pulsars

M. Marelli, A. De Luca, and P. Caraveo

INAF - Istituto di Astrofisica Spaziale e Fisica Cosmica Milano, via E. Bassini 15, 20133 Milano, Italy, e-mail: marelli@lambrate.inaf.it

Abstract. Using archival as well as freshly acquired data, we assess the X-ray behaviour of the *Fermi*/LAT γ-ray pulsars listed in the Second *Fermi* pulsar catalog, focussing on the distance-indipendent γ to X-ray flux ratios.
We collected photons from all the public observations that overlap the error box of *Fermi* pulsars by all the major observatories currently operating in the soft X-ray band: *Chandra/ACIS*, *XMM-Newton*, *SWIFT/XRT* and *Suzaku*. We re-analyzed all the X-ray data in order to follow an homogeneous procedure.
We obtained that pulsars with similar energetics have F_{γ}/F_X spanning 3 decades. Such spread is most probably stemming from vastly different geometrical configurations of the X and γ-ray emitting regions. With a 3σ confidence level, we can also conclude that the young radio-quiet (RQ) and young radio-loud (RL) datasets we used are somewhat different; similarly our RQ and millisecond (MS) pulsars' populations are different at a 5σ confidence level. On average, MS pulsars have the smallest F_{γ}/F_X values while RQ pulsars the highest. In particular all MS pulsars have lesser values of F_{γ}/F_X than all the RQ ones.

Key words. gamma rays: general, x rays: general, pulsars: general, stars: neutron

1. Introduction

The X-ray band can yield crucial information on the pulsar physics, fundamental to model both the thermal emissions and the non-thermal one, and tracing the presence of pulsar wind nebulae (PWNe).

Chandra's exceptional spatial resolution made it possible to discriminate clearly the PWN and the PSR contributions while *XMM-Newton*'s high spectral resolution and throughput unvealed the multiple spectral components which characterize pulsars (see e.g. Possenti et al. 2002); in particular, the non-thermal component seen in the X-rays seems reminescent of the spectral shape in the γ-ray band (see e.g. Kaspi et al. 2004) although the extrapolation of the X-ray spectra cannot account for the γ-ray fluxes (see e.g. Abdo et al. 2010b).

The *Fermi* Large Area Telescope (LAT) changed dramatically the high-energy pulsars' scenario estabilishing RQ pulsars as a major family of γ-ray emitting neutron stars. After three years of all-sky monitoring *Fermi*/LAT has detected 117 γ-ray pulsars, half of which are radio quiet (or - at least - radio faint) (Abdo et al. 2013). Containing roughly equal number of RL, RQ and MS pulsars the Fermi sample provides, for the first time, the possibility to compare the phenomenology of the three groups of pulsars assessing their similarities and their differences (if any).

Send offprint requests to: M. Marelli

2. X-ray analysis

We consider all γ-ray pulsars reported in the second *Fermi* pulsar catalog (Abdo et al. 2013). Our sample comprehends 117 pulsars of which 34 are RQ, 43 RL and 40 MS.

To assess the non-thermal X-ray spectra of Fermi pulsars, we used photons with energy 0.3<E<10 keV collected by all the major observatories currently operating in the soft X-ray band: *Chandra/ACIS* (Garmire et al. 2003), *XMM-Newton* (Struder et al. 2001; Turner et al. 2001), *SWIFT/XRT* (Burrows et al. 2005) and *Suzaku* (Mitsuda et al. 2007). We selected all the public observations that overlap the error box of *Fermi* pulsars or the Radio coordinates.

Differently from the γ-ray band, the X-ray coverage of *Fermi/LAT* pulsars is uneven since the majority of the newly discovered RQ PSRs have never been the target of a deep X-ray observation, while for other well-known γ-ray pulsars - such as Crab, Vela and Geminga - one can rely on a lot of observations. To account for such an uneven coverage, we classify the X-ray spectra on the basis of the available public X-ray data, thus assigning: label "0" to pulsars with no confirmed X-ray counterparts (or without a non-thermal spectral component); label "1" to pulsars with a confirmed counterpart but too few photons to assess its spectral shape; label "2" to pulsars with a confirmed counterpart for which the data quality allows for the analysis of both the pulsar and the nebula (if present). Moreover, we consider an X-ray counterpart to be confirmed if: X-ray pulsation has been detected, or X and Radio coordinates coincide, or X-ray source position has been validated through the blind-search algorithm developed by the Fermi collaboration (Ray et al. 2011) down to a few arcsecs error box. Though we are aware that a spatial coincidence with a serendipitous source is possible, as a rough estimate and according to X-ray LogN/LogS source distribution at low/intermediate galactic latitude (Novara et al. 2006), we evaluated the probability of finding a background source located inside a typical *Chandra* error box less than 0.0005. Such a probability raises of a factor ~50 when we rely only on *Suzaku* observations due to the much worse spatial sensitivity of the telescope. According to our classification scheme, we have 50 type-0, 11 type-1 and 56 type-2 pulsars. In total 67 γ-ray neutron stars (30 RLP, 19 MSP and 18 RQP) have an X-ray counterpart.

Since the X-ray observation database is continuously growing, the results available in literature encompass only fractions of the X-ray data now available. Moreover, they have been obtained with different versions of the standard analysis software or using different techniques to account for the PWN contribution. Thus, with the exception of the well-known and bright X-ray pulsars, such as Crab or Vela, we re-analyzed all the X-ray data publicly available following an homogeneous procedure. For each type-2 pulsar, we took into account the PWN contribution. First we searched the literature for evidence, if any, of the presence of a PWN and, if nothing was found, we analyzed the data to search for extended emission through a radial brilliance study If no evidence for the presence of a PWN was found, we extracted photons from circular regions containing ~95% of the pointlike source counts: about 2" for *Chandra*/ACIS, 20" for *XMM-Newton* and *Swift* and 1.3' for *Suzaku*. A case-by-case evaluation of the background could slightly change these extraction radii. All the datasets were then simultaneously fitted. On the other hand, if a PWN was present, its contribution was evaluated as follows. If the statistic was good enough, we simultaneously fitted spectra from the inner region, containing both PSR and PWN, and spectra from the extended region surrounding it. The inner region spectra were described by two absorbed (PWN and PSR) powerlaws (plus, eventually, a blackbody), while the outer ones by a single (PWN) powerlaw; the N_H and the PWN photon index values were linked in the two (inner and outer) spectra.

All the PSRs and PWNs have been described with absorbed powerlaws; when statistically needed, a blackbody component has been added to the pulsar spectrum. Absorption along the line of sight has been obtained through the fitting procedure but for pulsars with very low statistics we used values derived from observations taken in different bands.

For pulsars with a confirmed counterpart but too few photons to discriminate the spectral shape (type 1), we evaluated the unabsorbed flux by assuming a single powerlaw spectrum with a photon index of 2 to describe PSR+PWN, with an absorbing column obtained by rescaling the galactic one (http://heasarc.gsfc.nasa.gov/cgi-bin/Tools/w3nh/w3nh.pl) for the distance (Abdo et al. 2013).We also assumed the PWN and PSR thermal contributions to be 30% of the total source flux (a sort of mean value of all type 2 pulsars considered). For pulsars without a confirmed counterpart we evaluated an upper limit unabsorbed X-ray flux. We assumed a single powerlaw spectrum with a photon index of 2 to describe PSR+PWN and the column density has been set as above. The upper limit was evaluated as the flux yielding a signal-to-noise of 3.

Details on the reduction and fit of the data for each telescope, describing the tools we used for each telescope, the cross-calibration studies and the counterpart detection and the spectral fitting procedures, are provided in Marelli et al. (2011); Marelli (2012). Spectral results for each pulsar are reported in Marelli (2012); Abdo et al. (2013).

3. Discussion and conclusions

The X-ray luminosity, L_X, is correlated with the pulsar spin-down luminosity $\dot{E}$ (see e.g. Possenti et al. 2002). We are now facing a different panorama, since our ability to evaluate pulsars' distances has improved and we are now much better in discriminating pulsar emission from its nebula. For a detailed study of the X-ray luminosities see Marelli (2012). Similarly, the γ-ray luminosity, L_γ, is roughly correlated with the pulsar spin-down luminosity $\dot{E}$ through a double-linear relationship (see e.g. Marelli et al. 2011), expected in many theoretical models (see e.g. Zhang et al. 2004; Muslimov&Harding 2003) and it's shortly discussed in the *Fermi* LAT catalogue of γ -ray pulsars (Abdo et al. 2010a).

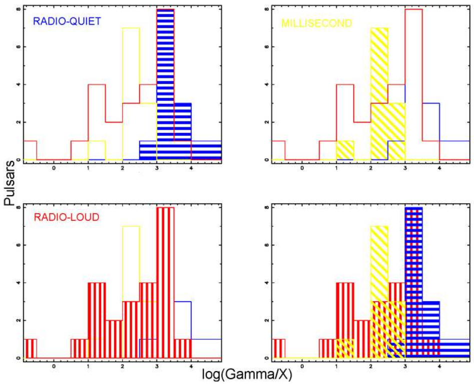

Fig. 1. $\log(F_\gamma/F_X)$ histogram. The step is 0.5; horizontal lines: RL pulsars; oblique lines: MS pulsars; vertical lines: RQ pulsars. Only high confidence pulsars (type 2) have been used.

At variance with the X-ray and γ-ray luminosities, the ratio between the X-ray and γ-ray luminosities is independent from pulsars' distances. This makes it possible to significatively reduce the error bars leading to more precise indications on the pulsars' emission mechanisms.

Figure 1 reports the histogram of the F_γ/F_X values using only type 2 (high quality X-ray data) pulsars. The RL pulsars have $< log(F_\gamma/F_X) >= 2.373$, the RQ population has $< log(F_\gamma/F_X) >= 3.484$ while the MS pulsars have $< log(F_\gamma/F_X) >= 2.310$ (see Table 1 for the main statistical parameters of the logs of F_γ/F_X). Applying the Kolmogoroff-Smirnov test to type 2 pulsars' $\log(F_\gamma/F_X)$ values we obtained that the chance for the RQ and RL datasets belong to the same population is 0.000357. Similarly, the KS test applied on MS and RQ type-2 pulsars give a probability of 1.9 $\times 10^{-7}$. We can conclude, with a 3σ confidence level, that the RQ and RL datasets we used are somewhat different; with a 5σ confidence level, we can say that our RQ and millisecond pulsars' populations are different. On average, MS pulsars have the smallest F_γ/F_X values. In particular all MS pulsars have lesser values of F_γ/F_X than all the RQ ones. Recently, it has been argued that some MSPs would have co-located radio and γ emitting regions, similar to some high-$\dot{E}$, young γ-ray pulsars (Abdo et al.

Table 1. Main statistical parameters of $\log(F_\gamma/F_X)$ values for the three type 2 pulsars' populations.

Pop	Min Value	Max Value	Mean	St.Dev.
RQ	2.824	4.810	3.484	0.491
MS	1.324	2.740	2.310	0.480
RL	-0.529	3.708	2.373	1.108

2010c; Ravi et al. 2010). However, other millisecond pulsars don't show such a co-location of the two emitting regions so that we cannot easily use this to explain the low F_γ/F_X values measured for out entire MS sample. Anyway, the apparent inconsistency we find between RQ and MS pulsars makes more and more interesting future studies on RQ MS pulsars **(if any)**.

Figure 1 clearly shows the scatter on the F_γ/F_X parameter values, also for a given value of $\dot{E}$. Such an apparent spread cannot obviously be ascribed to a low statistic nor is related to distance uncertainties. Such a scatter can be due to geometrical effects. For both X-ray and γ-ray energy bands:

$$L_{\gamma,X} = 4\pi f_{\gamma,X} F_{obs} D^2 \qquad (1)$$

where f_X and f_γ account for the X and γ beaming geometries (which may or may not be related) and depend only from the viewing angle and the magnetic inclination of the pulsar (Watters et al. 2009). With an high Than, the very important scatter found for F_γ/F_X values can be due to the different geometrical configurations which determine the emission at different wavelength of each pulsar. While geometry is clearly playing an equally important role in determining pulsar luminosities, the F_γ/F_X plot makes its effect easier to appreciate.

A complete study of the selection effects playing a role in this relationship are reported in Marelli (2012). They concluded that the γ-ray selection introduced no changes in the two populations, while the X-ray selection excluded objects both faint and/or far away; any distortion, if present, is not overwhelming. The observational panorama is quickly evolving. The γ-ray pulsar list is continuously growing and this triggers more X-ray observations, improving both in quantity and in quality the database of the neutron stars detected in X and γ-rays to be used to compute our multiwavelength, distance independent study. However, to fully exploit the information packed in the F_γ/F_X a complete 3D modeling of pulsar magnetosphere is needed to account for the different locations and heights of the emitting regions at work at different energies. Such modeling could provide the clue to account for the spread we have observed for the ratios between γ and X-ray fluxes as well as for the systematically higher values measured for RQ pulsars.

References

Abdo, A.A. et al., 2010, ApJ, 187, 460
Abdo, A.A. et al., 2010 ApJ, 712, 1209
Abdo, A.A. et al., 2010 ApJ, 712, 957
Abdo, A.A. et al., 2013, in preparation (the 2nd pulsar catalogue)
Burrows, D. N. et al., 2005, Space Sci. Rev., 120, 165
Garmire, G.G. et al., 2003, SPIE 4851, 28
Kaspi, V.M. et al., 2004, astro.ph. 2136K
Marelli, M. et al. 2011, ApJ, 733, 82
Marelli, M. 2012, arXiv:1205.1748
Mitsuda, K., et al. 2007, PASJ, 59, 1
Muslimov, A.G. & Harding, A.K., 2003, ApJ, 588, 430
Novara, G., et al., 2006, A&A 448, 93
Possenti, A. et al., 2002, A&A, 387, 993
Ravi, V. et al., 2010, ApJ, 716, 85
Ray, P.S. et al., 2011, ApJS, 194, 17
Struder, L. et al., 2001, A&A, 365, L18
Turner, M.J.L. et al. 2001, A&A, 365, L27
Watters, K.P. et al., 2009, ApJ, 695, 1289
Zhang, L. et al., 2004, ApJ, 604, 317